

Production, Purification, and Initial Crystallization of Recombinant Epidermal Growth Factor Receptor Tyrosine Kinase Domain (EGFR-TKD) as a Structural Basis for Future Drug Screening Studies

Edanur Topalan¹, Halil İbrahim Çiftçi^{2,3,4}, Hasan Demirci^{1,5✉}

¹Department of Molecular Biology and Genetics, Koc University, 34450, İstanbul, Türkiye,

²Medicinal and Biological Chemistry Science Farm Joint Research Laboratory, Faculty of Life Sciences, Kumamoto University, Kumamoto 862-0973,

³Department of Drug Discovery, Science Farm Ltd., Kumamoto 862-0976, Japan,

⁴Department of Molecular Biology and Genetics, Mehmet Akif Ersoy University, Burdur 15030, Türkiye,

⁵Stanford PULSE Institute, SLAC National Laboratory, Menlo Park, California, United States of America

¹  <https://orcid.org/0009-0009-0532-020X>, ^{2,3,4}  <https://orcid.org/0000-0002-9796-7669>, ^{1,5}  <https://orcid.org/0000-0002-9135-5397>

✉: hdemirci@ku.edu.tr

ABSTRACT

The epidermal growth factor receptor tyrosine kinase domain (EGFR-TKD) is a key regulator of intracellular signaling events that control cell proliferation. Aberrant EGFR activation is closely associated with the development of non-small cell lung cancer (NSCLC). In this study, recombinant EGFR-TKD was expressed in *Escherichia coli* Rosetta™ 2 (DE3) cells using a pET28a(+) expression plasmid carrying an N-terminal 6×His-SUMO-tag. During expression, a large proportion of the protein accumulated in inclusion bodies; therefore, we employed a solubilization approach. Treatment with 1.5% sarcosyl reproducibly yielded a soluble protein fraction compatible with subsequent purification steps. Optimizing induction parameters, including temperature, IPTG concentration, and expression duration, improved both the yield and solubility of the protein. Following size-exclusion chromatography, the monomeric protein fraction was isolated and used for crystallization trials, which resulted in the formation of small but well-defined microcrystals under several conditions. Although these crystals did not yet provide diffraction suitable for structure determination, their reproducible appearance indicates that the obtained EGFR-TKD is structurally competent for crystallization trials. Overall, the workflow establishes a practical and reproducible bacterial expression and purification strategy that forms a basis for continued crystallization optimization and structure-based inhibitor development targeting EGFR-driven cancers.

Key words: EGFR, sarcosyl, *E. coli*, crystallization, drug discovery.

Epidermal Growth Factor Receptor Tirozin Kinaz Domaini'nin (EGFR-TKD) Rekombinant Üretimi, Saflaştırılması ve İlk Kristalleştirilmesi: İlaç Taraması Çalışmaları İçin Yapısal Bir Temel

Öz

Epidermal Büyüme Faktörü Rezeptörü Tirozin Kinaz Domaini (EGFR-TKD), hücresel sinyal iletimi ve proliferasyon merkezinde yer alan kritik bir düzenleyici proteindir. EGFR aktivitesinin düzensizliği, özellikle küçük hücreli dışı akciğer kanseri (KHDAK) olmak üzere çeşitli kanserlerin gelişimi ve ilerlemesiyle yakından ilişkilendirilmiştir. Bu çalışmada, EGFR-TKD proteini, N-uçta 6×SUMO etiketi taşıyan pET28a(+) ekspresyon plazmidi kullanılarak *Escherichia coli*'de üretildi. Üretilen proteinin büyük kısmı inklüzyon cisimciklerinde birikmiş olup, %1,5 sarcosil kullanılarak etkin bir şekilde çözünür hale getirilmiş ve kristalizasyon denemeleri için uygun bir fraksiyon olarak toplanmıştır. İndüksiyon sıcaklığı, IPTG konsantrasyonu ve ekspresyon süresinin optimize edilmesiyle protein verimi ve çözünürlüğü artırıldı. Saflaştırılan protein örneği belirli koşullar altında başlangıç

düzeyinde mikrokristaller oluşturdu. Bu yöntem, yapısal çalışmalar için düşük maliyetli ve tekrarlanabilir bir bakteriyel ekspresyon sistemi sağlamaktadır. Çalışma, EGFR kaynaklı kanserleri hedefleyen yapı temelli ilaç geliştirme çalışmalarına yönelik ileri kristalizasyon optimizasyonu için bir temel oluşturmaktadır.

Anahtar kelimeler: EGFR, sarkozil, *E. coli*, kristalizasyon, ilaç keşfi

INTRODUCTION

Receptor tyrosine kinases (RTKs) are key mediators of intercellular signaling that coordinate cell proliferation, differentiation, and survival by phosphorylating downstream effectors. Their activation regulates essential biological processes, including tissue growth, repair, and homeostasis, and disruptions in these pathways are strongly associated with oncogenesis (Lemmon & Schlessinger, 2010; Roskoski, 2014). Within this group, the Epidermal Growth Factor Receptor (EGFR) belongs to the ErbB receptor family alongside HER2 (human epidermal growth factor receptor 2), HER3 (human epidermal growth factor receptor 3), and HER4 (human epidermal growth factor receptor 4), all of which have critical roles in epithelial cell signaling and tumor progression (Yarden & Sliwkowski, 2001; Yarden & Pines, 2012; Hubbard, 1999).

EGFR activation begins with ligand binding to its extracellular region, which triggers conformational changes that promote receptor dimerization and autophosphorylation in the tyrosine kinase domain (TKD) (Harris et al., 2003; Ferguson et al., 2003). The resulting phosphorylation events initiate several downstream cascades, including MAPK, PI3K/AKT, and JAK/STAT pathways, thereby influencing gene expression and cell fate decisions. The capacity of EGFR to form both homo- and heterodimers with other ErbB family members adds additional layers of signaling diversity and regulatory complexity (Lenferink, 1998; Niggenaber et al., 2020).

Mutations in the EGFR tyrosine kinase domain (TKD) represent some of the most clinically significant oncogenic drivers in non-small cell lung cancer (NSCLC), which accounts for approximately 85% of lung cancer cases worldwide (Johnson et al., 2022; Morgillo et al., 2016; Zhao et al., 2021). Activating mutations such as exon 19 deletions and L858R substitutions stabilize EGFR in its active conformation, resulting in constitutive signaling and uncontrolled proliferation. First-generation tyrosine kinase inhibitors (TKIs), including gefitinib and erlotinib, provided targeted therapeutic strategies for these mutations, but secondary alterations—particularly T790M and C797S—frequently lead to drug resistance and disease relapse (Mansour et al., 2023; Das et al., 2024; Westover et al., 2018). Moreover, exon 20 insertions comprise a rarer but clinically important subset of EGFR alterations that respond poorly to conventional TKIs (Oxnard et al., 2013; Brazel et al., 2022).

To address these challenges, current research focuses on fourth-generation inhibitors and combination strategies, including bispecific antibody–TKI regimens such as amivantamab–lazertinib, which has demonstrated promising outcomes in treatment-naïve EGFR-mutant NSCLC (Cho et al., 2024). Efforts to develop inhibitors targeting rare or compound EGFR mutations continue to expand, reflecting the ongoing progression of personalized oncology (Gou et al., 2024; Das et al., 2021; Wang et al., 2024). At the same time, advances in structural biology and computational modeling have provided detailed insights into EGFR-TKD conformational dynamics, informing rational inhibitor design and improved therapeutic strategies (Eck & Yun, 2010; Jura et al., 2009).

Despite these advancements, obtaining soluble and functional EGFR-TKD from recombinant expression in *E. coli* remains challenging, largely due to aggregation and the tendency of the protein to accumulate in inclusion bodies (Elloumi-Mseddi et al., 2013). Therefore, effective solubilization and refolding strategies are essential for preparing material suitable for structural studies and, in particular, for producing crystals with sufficient order for diffraction. The microbatch crystallization method, which has previously been applied to other RTKs, provides a potential route to help overcome these bottlenecks. In addition, structural studies on other members of the ErbB family, including HER2, have informed our experimental strategy for the expression, purification, and crystallization of EGFR-TKD (Topalan et al., 2025; Sever et al., 2019).

To date, numerous small-molecule inhibitors have been developed against EGFR, several of which show promising efficacy in NSCLC. Within this context, our research group has focused on the rational design, synthesis, and biological evaluation of pyrazoline–thiazole hybrid compounds as potential anti-NSCLC agents with notable EGFR inhibitory activity (Sever et al., 2019; 2025; Çiftçi et al., 2024; Reymova et al., 2025).

Compound I (Sever et al., 2019) (Figure 1) demonstrated notable anti-NSCLC activity, exhibiting an IC_{50} (half maximal inhibitory concentration) value of 10.76 μ M, which was superior to that of erlotinib (IC_{50} = 22.35 μ M). In addition, compound I showed remarkable EGFR inhibition with an IC_{50} value of 4.34 μ M. Subsequently, naphthyl-substituted pyrazoline–thiazole hybrids were evaluated for their anti-NSCLC potential, and compound II (Çiftçi et al., 2024) (Figure 1) displayed potent cytotoxic activity with an IC_{50} value of 9.51 μ M, outperforming lapatinib (IC_{50} = 16.44 μ M). Compound II also inhibited EGFR by 58.32% at 10 μ M.

In our further investigations (Reymova et al., 2025; Sever et al., 2025), the precursor compounds of the pyrazoline–thiazole hybrids, namely B-4 and B-2, demonstrated stronger anti-NSCLC activity, with IC_{50} values of $20.49 \pm 2.71 \mu\text{M}$ and $2.14 \pm 0.83 \mu\text{M}$, respectively. These activities were higher than those of the most active reference compounds, compound III and compound IV, reported in the respective studies (Figure 1).

Moreover, both B-4 and B-2 exhibited substantial EGFR inhibitory activity at 10 μ M, with inhibition rates of 46% and 66%, respectively.

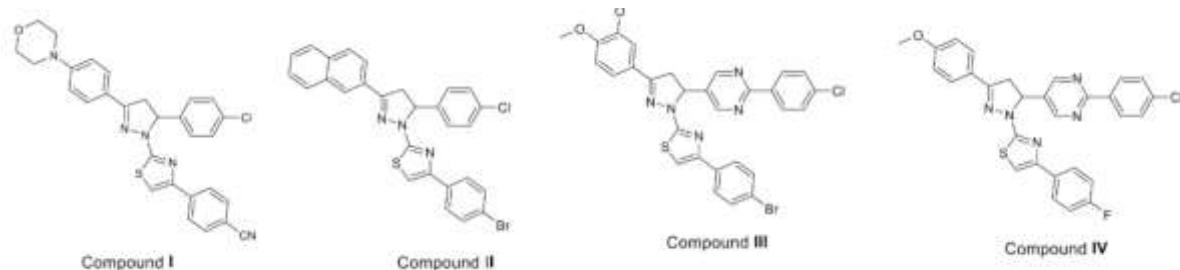


Figure 1. The chemical structures of compounds I-IV.

Therefore, this study aims to establish a reproducible and efficient workflow for the recombinant expression, purification, and crystallization of human EGFR-TKD. The resulting system provides a reliable structural basis for rational inhibitor screening and structure-guided drug discovery targeting NSCLC (Çiftçi et al., 2024; Reymova et al., 2025).

2. MATERIALS AND METHODS

Reagents and instruments

All chemicals, media components, and crystallization screens used in this study were obtained from commercial suppliers (Atalay et al., 2023). Antibiotics (ampicillin, chloramphenicol, and kanamycin), IPTG, and Ni-NTA resin were purchased from GoldBio and Qiagen. Other laboratory-grade reagents, including glycerol, NaCl, HCl, urea, and yeast extract, were supplied by ISOLAB and BD Biosciences. Imidazole was obtained from BioFroxx, while sarcosyl, SDS, Tris base, and Triton X-100 were purchased from Sigma-Aldrich. Paraffin oil was supplied by Tekkim Kimya, and Luria–Bertani (LB) agar and tryptone were procured from Caisson and BD Biosciences, respectively.

Protein purification and analysis were performed using AKTA GoFPLC chromatography systems (Cytiva), Beckman Coulter centrifuges (Allegra 15R, Avanti J-26S, and Optima™ L-80 XP ultracentrifuge), and a Branson W250 sonifier. Laboratory consumables included cryotubes, Eppendorf tubes, and Falcon tubes. Protein quality and purity were evaluated using the TGX-Mini Protean sodium dodecyl sulfate–polyacrylamide gel electrophoresis (SDS-PAGE) system (Bio-Rad). Crystallization trials were carried out with a variety of commercial screening kits. X-ray diffraction (XRD) data collection was performed using a Rigaku XtaLAB Synergy Flow XRD system (Turkish DeLight Home Source) (Figure 8), and purified proteins were analyzed using a Superdex™ 200 size exclusion column (Cytiva).

Gene construction and transformation

The plasmid construct containing the coding sequence of the human EGFR-TKD (UniProt ID: P00533, residues 696–1022) was obtained from GenScript (USA) (Elloumi-Mseddi et al., 2013). The gene sequence was cloned into the pET28a(+) vector with an N-terminal 6×His-SUMO-tag and ULP1 protease cleavage site. The plasmid was supplied ready-to-use and transformed into *E. coli* Rosetta™ 2 (DE3) competent cells.

Transformation procedure

Two microliters of plasmid DNA were mixed with 50 μ L of competent cells on ice for 20 min, heat-shocked at 42 °C for 45 seconds, and placed on ice for 2 min. After addition of 500 μ L LB medium, cells were incubated at 37 °C for 90 min. Fifty microliters of the culture were spread onto LB agar plates containing kanamycin (50 μ g/mL) and chloramphenicol (35 μ g/mL), and incubated overnight. Single colonies were selected and inoculated into LB broth for glycerol stock preparation.

Protein expression

Transformed *E. coli* cells were cultured in 4 L LB medium supplied with kanamycin and chloramphenicol. When the culture reached an OD₆₀₀ of approximately 0.8, expression was induced with 0.4 mM isopropyl β-D-1-thiogalactopyranoside (IPTG) for 4 h at 37 °C following induction. Cells were harvested by centrifugation and stored at -45 °C.

Protein purification and tag removal

Cell pellets were lysed in buffer (10 mM Tris-HCl, 150 mM NaCl, 1 mM PMSF, 5 mM β-mercaptoethanol, 1.5% sarcosyl, pH 8.0) and disrupted by sonication. The lysate was clarified by ultracentrifugation and subjected to SEC on a Superdex 200 column. Fractions were monitored at 280 nm (Figure 2) and analyzed by SDS-PAGE (Figure 3).

SDS-PAGE analysis

Samples collected from different stages of the purification process were analyzed by SDS-PAGE (Figures 4–6). SDS-PAGE was performed on 12% gels, followed by visualization using Coomassie Brilliant Blue staining.

Crystallization

Crystallization was carried out by the sitting-drop microbatch method (Atalay et al., 2023). Equal volumes (0.83 μL + 0.83 μL) of protein and precipitant were mixed and covered with paraffin oil. More than 3000 screening conditions were tested (Table 1).

Table 1. A list of the crystallization screening conditions used in this study.

Natrix I	Wiz Synergy IV
Natrix II	Pact Premier I
Wizard I	Pact Premier II
Wizard II	PEG Ion I
Wizard III	PEG Ion II
Wizard IV	Salt RX I
Crystal Cryo I	Salt RX II
Crystal Cryo II	Proplex I
Crystal Screen I	Proplex II
Crystal Screen II	MembFAC
Crystal Screen II	Crystal Lite
Wizard Cryo I	PEG RX I
Wizard Cryo II	PEG RX II
Helix I	Multi XTAC
Helix II	Macro SOL
Midas I	3D Structure Screen

Midas II	Stura Footprint
NR-LBD I	Clear Strategy Screen I & II (pH 4.5)
NR-LBD II	Clear Strategy Screen I & II (pH 5.5)
PGA-LM I	Clear Strategy Screen I & II (pH 6.5)
PGA-LM II	Clear Strategy Screen I & II (pH 7.5)
Morpheus I	Clear Strategy Screen I & II (pH 8.5)
Morpheus II	Quick Screen / Ionic Liquid Screen
Structure I	GRID/NaCl – Na Malonate (*)
Structure II	GRID/PEG 6000–Ammonium Sulfate(*)
Index I	GRID/MPD – PEG LiCl (*)
Index II	JENA BC Nuc Pro 1/2
Wiz Synergy I	JENA BC Nuc Pro 3/4
Wiz Synergy II	JCSG-I
Wiz Synergy III	JCSG-II

The table shows a variety of commercial and specialized crystallization screens, each designed to test a wide range of conditions for optimal protein crystallization. These screens include a variety of chemical components such as salts, PEG, and pH variations, as well as cryocrystallography and ionic liquid screening conditions. The screens are intended to help identify the most favorable conditions for obtaining high-quality protein crystals, allowing for subsequent structural analysis using X-ray diffraction.

Initial crystals formed in 1.4 M lithium sulfate, 0.1 M Bis-Tris (pH 6.5), and additional crystals in 0.25 M potassium thiocyanate, 27% PEG 3350, pH 6.9 (Figures 9-10).

RESULTS AND DISCUSSION

Expression and solubilization

The recombinant EGFR-TKD was successfully expressed in *E. coli* Rosetta™ 2 (DE3) cells and localized predominantly in the insoluble fraction, consistent with inclusion body formation. The aggregated protein fraction was efficiently solubilized with 1.5% sarcosyl, recovering the active protein for subsequent purification steps.

The overall architecture and catalytic organization of EGFR-TKD is consistent with the general framework described for RTKs, including the conserved activation loop and regulatory motifs responsible for autoinhibition (Hubbard, 1999). The recovery of soluble EGFR-TKD from inclusion bodies using 1.5% sarcosyl suggests that mild detergents can effectively aid in solubilization without disrupting the structural features required for catalytic function. This observation is consistent with earlier reports describing detergent-assisted refolding strategies for other RTKs (Elloumi-Mseddi et al., 2013).

Purification and tag removal

SEC profiling showed that the protein eluted primarily as a monomeric species, and this fraction was selected for subsequent crystallization experiments (Figure 2). The purity of the isolated protein was assessed by SDS-PAGE, where the target band appeared as a distinct and well-defined signal at the expected molecular weight (Figure 3). SUMO-tag cleavage optimization results are shown in Figures 4-5, and the final purification outcomes are presented in Figure 6. Although sarcosyl enabled efficient solubilization of EGFR-TKD, it also

disrupted Ni-NTA affinity binding, consistent with previous findings on detergent interference. Therefore, SEC was preferred over Ni-NTA purification. This approach provided highly pure monomeric protein suitable for crystallization, validating the adaptability of the workflow for other ErbB receptor kinases.

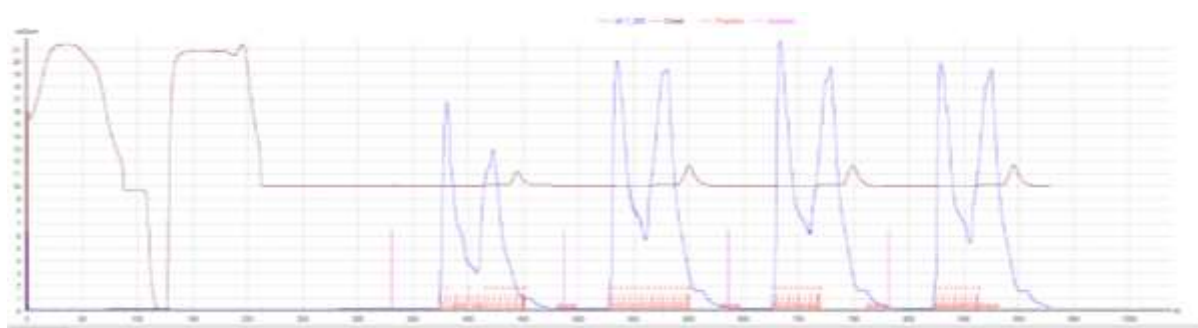


Figure 2. Size-Exclusion Chromatography (SEC) Analysis. SEC analysis of the EGFR-TKD protein reveals two distinct peaks. The first, larger peak corresponds to the monomeric form of the protein, while the second, smaller peak represents aggregated or multimeric species. The majority of the protein elutes as a monomer. The isolated monomeric fraction was used for further structural studies and crystallization trials.

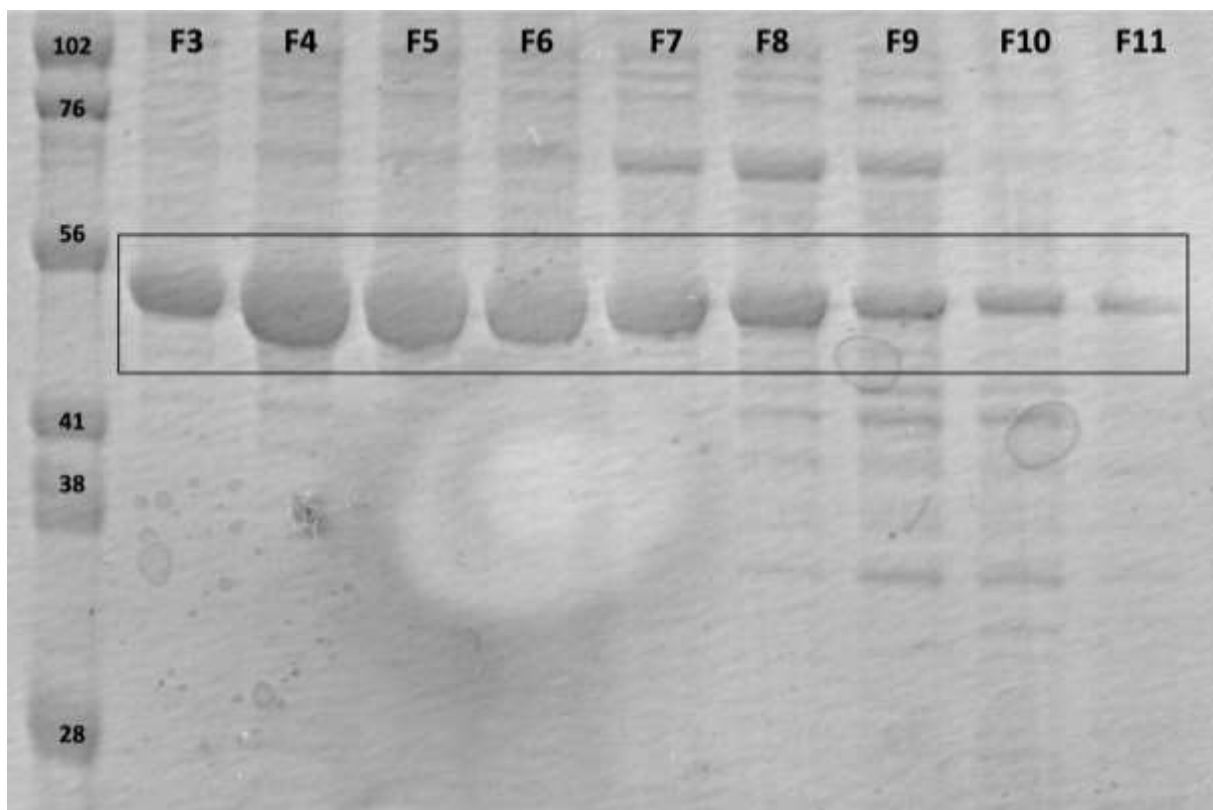


Figure 3. 12% SDS-PAGE analysis of SEC fractions.

Tag removal was performed using ULP1 protease (5:1000 v/v, 4 °C, 30 min). Cleavage efficiency was tested under various conditions (Figure 4), and the optimized ratio yielded complete removal (Figure 5). Reverse Ni-NTA affinity chromatography purification separated cleaved and uncleaved species (Figure 6). The final protein concentration was 2.4 mg/mL.

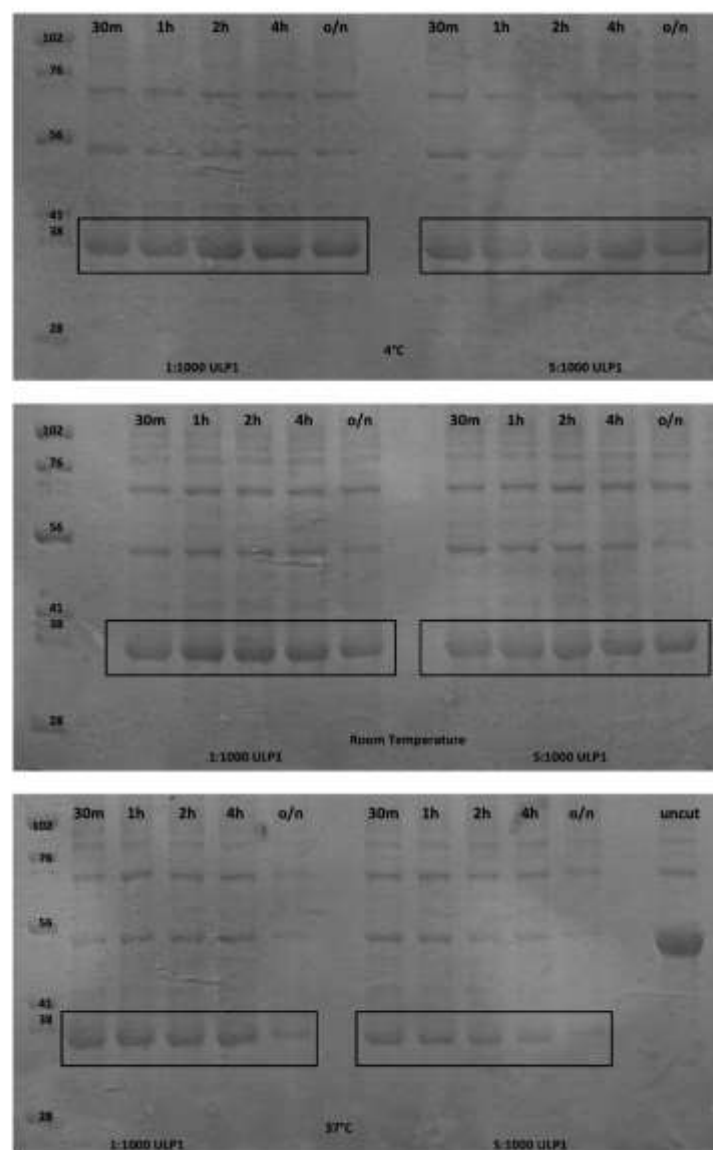


Figure 4. Cleavage analysis of SUMO-tagged EGFR-TKD using ULP1 protease at different enzyme-to-substrate (v/v) ratios (1:1000 and 5:100), temperatures (4°C, room temperature, and 37°C), and incubation times (30 min, 1 h, 2 h, 4 h, and overnight).

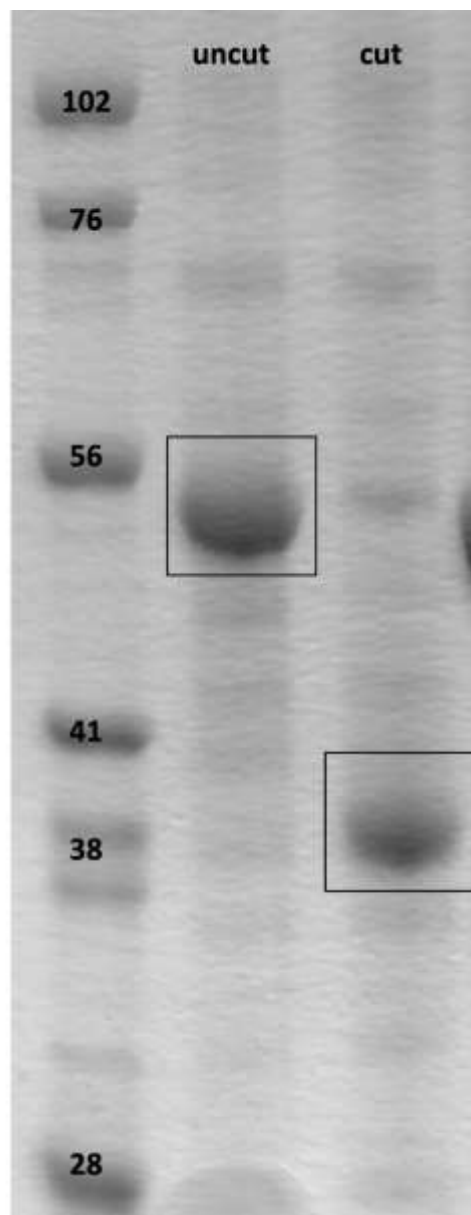


Figure 5. 12% SDS-PAGE analysis of SUMO-tag cleavage 5:1000 ULP1 at 4°C for 30 min.

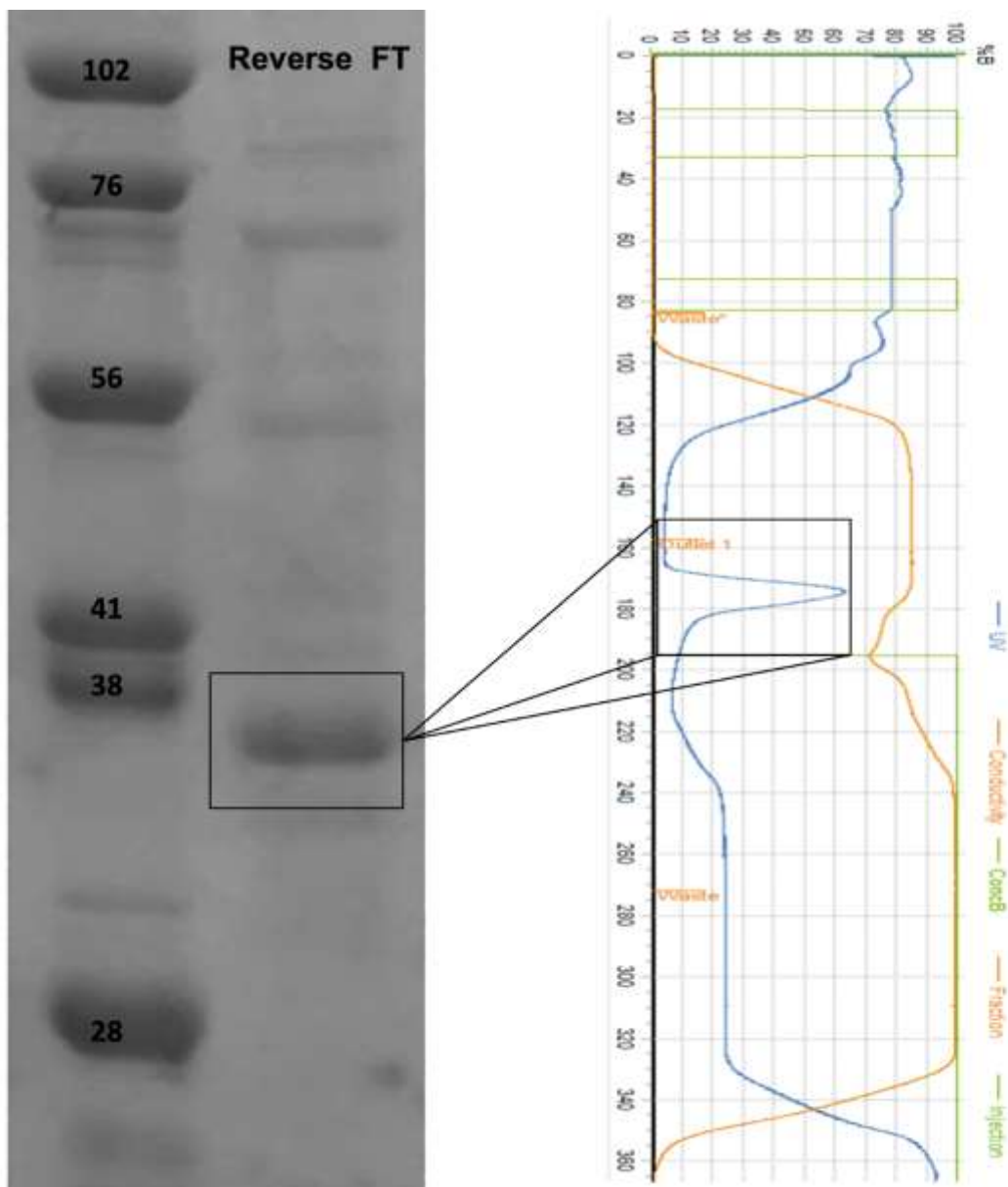


Figure 6. EGFR-TKD tag removal via Ni-NTA affinity chromatography results and flow-throughs of the concentrated sample (2.4 mg/mL) analyzed on a 12% SDS gel.

Crystallization results

Crystallization screening resulted in the formation of small, well-defined crystals under multiple conditions (Table 1; Figures 7, 9–10). Diffraction experiments were carried out using the Turkish DeLight XRD system (Figure 8), confirming the presence of ordered crystalline material. The repeated appearance of microcrystals across different conditions indicates that the purified EGFR-TKD preparation is suitable for crystallization, although further optimization is required to improve crystal size and quality.

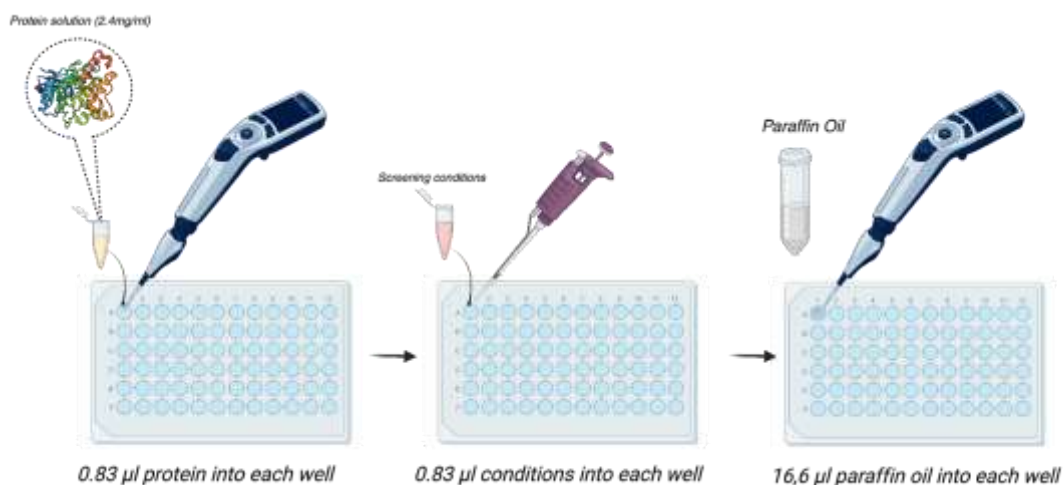


Figure 7. Crystallization workflow.

The generation of microcrystals is consistent with previous structural studies on EGFR and other ErbB family kinases, in which conformational flexibility of the kinase domain has been shown to influence crystallization behavior and lattice formation (Jura et al., 2011; Roskoski, 2019). In such systems, additional stabilization strategies are often required to obtain larger and more ordered crystals. Recent reviews continue to emphasize the conformational complexity of EGFR kinase regulation and the importance of stabilization strategies in structural studies (Topalan et al., 2025).

Ligand binding is known to stabilize specific kinase conformations and has frequently been employed to improve crystallization outcomes for EGFR and related kinases (Roskoski, 2019). Accordingly, the microcrystals obtained in the present study represent a suitable starting point for further optimization through co-crystallization with reference inhibitors.

Taken together, these results demonstrate that the established expression, purification, and crystallization workflow yields reproducible EGFR-TKD microcrystals. Future efforts will focus on optimizing crystallization parameters and incorporating ligand-based stabilization strategies to obtain crystals suitable for high-resolution structural analysis.



Figure 8. Rigaku XtaLAB Synergy Flow XRD system (Turkish DeLight Home Source XRD)

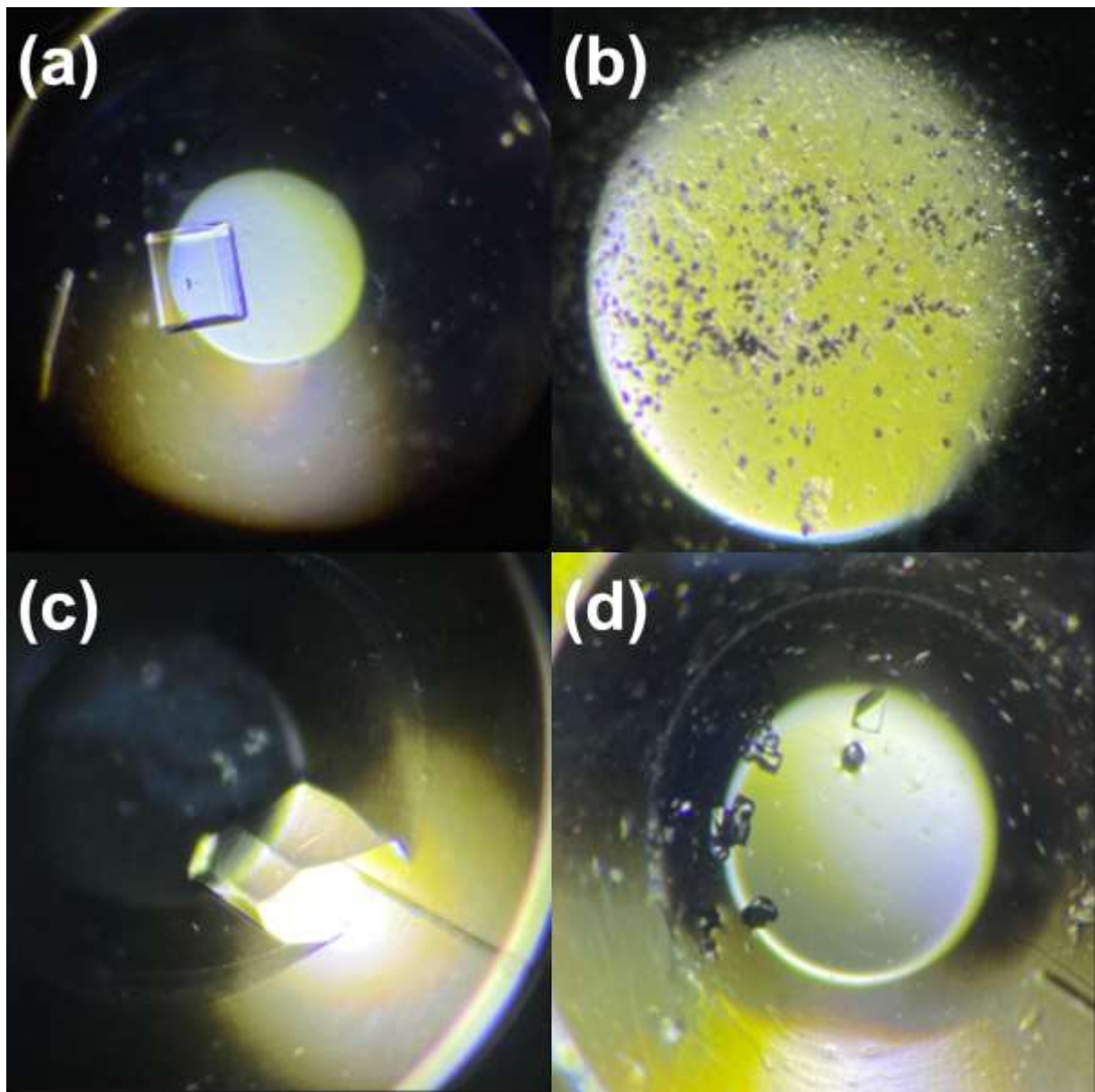


Figure 9. Crystal photos (a) EGFR-TKD Crystal Cryo-II #29, (b) EGFR-TKD Index-II #16, (c) EGFR-TKD NR-LBD-II #42, (d) EGFR-TKD Grid/NaCl/Na Malonate #18

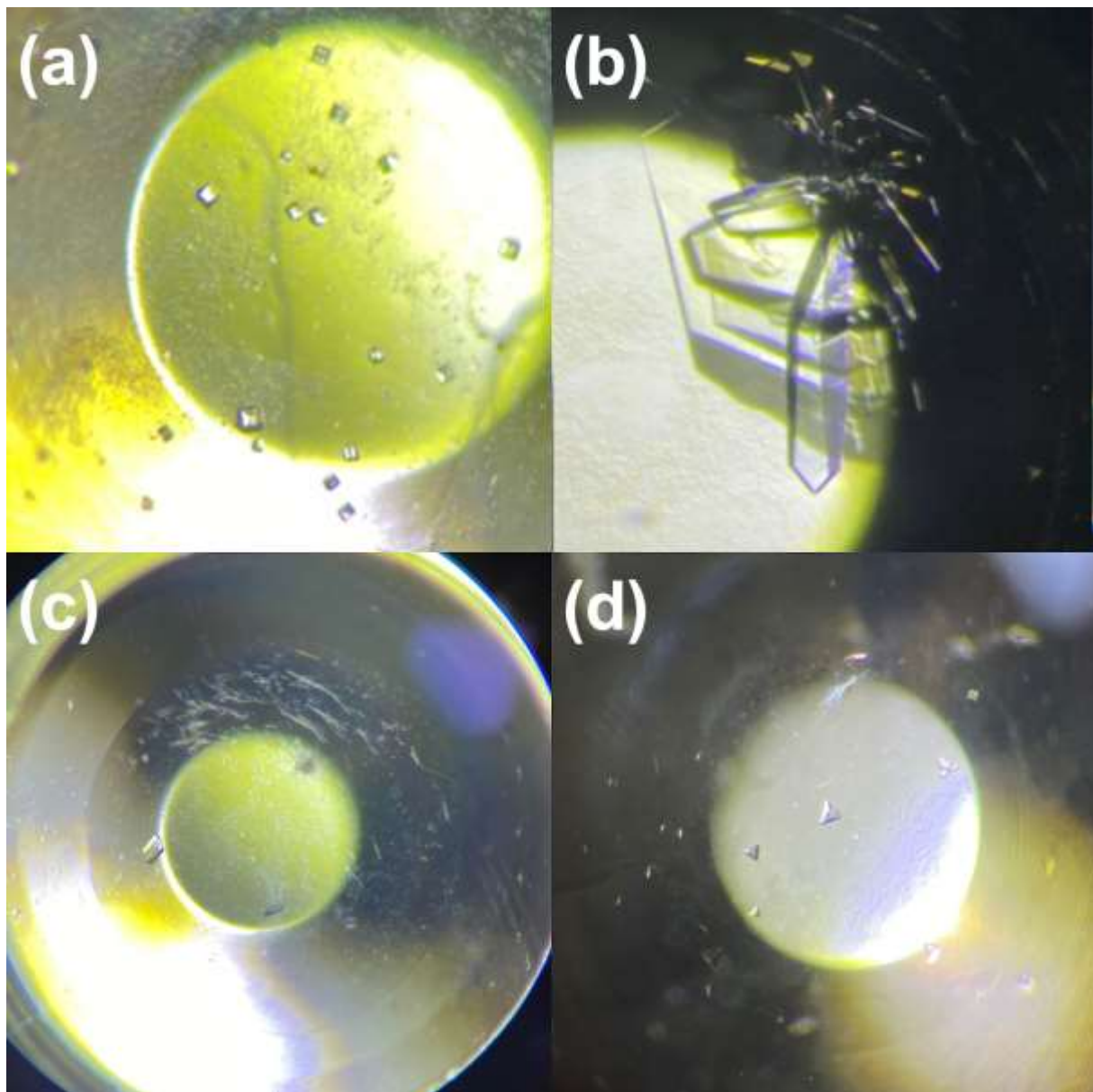


Figure 10. Crystal photos (a) EGFR-TKD+Reference Drug Helix-I #22, (b) EGFR-TKD NR-LBD-II #41, (c) EGFR-TKD+Erlotinib Helix-I #32, (d) EGFR-TKD+Erlotinib Wizard Cryo-I #3

CONCLUSION

In this study, we established a practical and reproducible workflow for the recombinant expression and crystallization of EGFR-TKD in *E. coli*. Although the protein exhibited a tendency to accumulate in inclusion bodies, solubilization with 1.5% sarcosyl consistently yielded a soluble fraction that could be purified and applied to crystallization screening. These results demonstrate that a bacterial expression system can provide structurally competent EGFR-TKD samples without reliance on eukaryotic expression platforms, offering an accessible basis for continued optimization and structural studies.

The reproducible formation of initial microcrystals confirms the feasibility of the developed approach and provides a solid foundation for further refinement of crystallization conditions. The established workflow therefore represents an important step toward generating crystallizable EGFR-TKD suitable for structure-based drug discovery efforts.

Overall, this work contributes to the structural investigation of EGFR and establishes a robust experimental framework for future co-crystallization studies with kinase inhibitors. Ongoing and future studies will focus on improving crystal quality through ligand-assisted stabilization and extending this strategy to other members of the ErbB receptor family (Topalan et al., 2025; Das et al., 2024).

Acknowledgements

The authors thank Associate Professor Belgin Sever for her valuable contributions. The authors also acknowledge the assistance of A. Büyükgüngör, M. Çiğdem, and S. Güra during the experimental work. This study was supported by the Scientific and Technological Research Council of Türkiye (TÜBİTAK) under Grant No. 122Z775.

Declaration of interests

The authors declare that they have no known competing financial interests or personal relationships that could have appeared to influence the work reported in this paper

Author Contributions

Edanur TOPALAN: Conceptualization; data curation; formal analysis; investigation; methodology; software; writing—original draft; writing—review and editing.

Halil İbrahim ÇİFTÇİ: Conceptualization; data curation; formal analysis; funding acquisition; investigation; methodology; project administration; software; writing—original draft; writing—review and editing.

Hasan DEMİRCİ: Conceptualization; data curation; formal analysis; funding acquisition; investigation; methodology; project administration; software; writing—original draft; writing—review and editing.

ORCID

Edanur TOPALAN  <https://orcid.org/0009-0009-0532-020X>

Halil İbrahim ÇİFTÇİ  <https://orcid.org/0000-0002-9796-7669>

Hasan DEMİRCİ  <https://orcid.org/0000-0002-9135-5397>

Article History

Submission received: 16.10.2025

Revised: 06.12.2025

Accepted: 09.12.2025

REFERENCES

Atalay, N., Akcan, E. K., Gül, M., Ayan, E., Destan, E., Ertem, F. B., Tokay, N., Çakılkaya, B., Nergiz, Z., Karakadioğlu, G., Kepceoğlu, A., Yapıcı, İ., Tosun, B., Baldır, N., Yıldırım, G., Johnson, J. A., Güven, Ö., Shafiei, A., Arslan, N. E., ... Demirci, H. (2023). Cryogenic X-ray crystallographic studies of biomacromolecules at Turkish Light Source "Turkish DeLight". *Turkish Journal of Biology*, 47(1), 1–13. <https://doi.org/10.55730/1300-0152.2637>

Brazel, D., Kroening, G., & Nagasaka, M. (2022). Non-small cell lung cancer with EGFR or HER2 exon 20 insertion mutations: Diagnosis and treatment options. *BioDrugs*, 36(6), 717–729. <https://doi.org/10.1007/s40259-022-00556-4>

Cho, B. C., Lu, S., Felip, E., Spira, A. I., Girard, N., Lee, J.-S., Lee, S.-H., Ostapenko, Y., Danchaivijitr, P., Liu, B., Alip, A., Korbenfeld, E., Dias, J. M., Besse, B., Lee, K.-H., Xiong, H., How, S.-H., Cheng, Y., Chang, G.-C., Yoshioka, H., ... Hayashi, H. (2024). Amivantamab plus Lazertinib in previously untreated EGFR-mutated advanced NSCLC. *The New England Journal of Medicine*, 391(16), 1486–1498. <https://doi.org/10.1056/NEJMoa2403614>

Çiftçi, H., Otsuka, M., Fujita, M., & Sever, B. (2024). New naphthalene-linked pyrazoline–thiazole hybrids as prominent antilung and anti-breast cancer inhibitors. *Turkish Journal of Chemistry*, 48(6), 856–866. <https://doi.org/10.55730/1300-0527.3704>

Das, D., Wang, J., & Hong, J. (2021). Next-generation kinase inhibitors targeting specific biomarkers in non-small cell lung cancer (NSCLC): A recent overview. *ChemMedChem*, 16(16), 2459–2479. <https://doi.org/10.1002/cmdc.202100166>

Das, D., Xie, L., & Hong, J. (2024). Next-generation EGFR tyrosine kinase inhibitors to overcome C797S mutation in non-small cell lung cancer (2019–2024). *RSC Medicinal Chemistry*, 15(10), 3371–3394. <https://doi.org/10.1039/d4md00384e>

Eck, M. J., & Yun, C. H. (2010). Structural and mechanistic underpinnings of the differential drug sensitivity of EGFR mutations in non-small cell lung cancer. *Biochimica et Biophysica Acta (BBA) - Proteins and Proteomics*, 1804(3), 559–566. <https://doi.org/10.1016/j.bbapap.2009.12.010>

Elloumi-Mseddi, J., Jellali, K., & Aifa, S. (2013). In vitro activation and inhibition of recombinant EGFR tyrosine kinase expressed in *Escherichia coli*. The Scientific World Journal, 2013, 807284. <https://doi.org/10.1155/2013/807284>

Ferguson, K. M., Berger, M. B., Mendrola, J. M., Cho, H. S., Leahy, D. J., & Lemmon, M. A. (2003). EGF activates its receptor by removing interactions that autoinhibit ectodomain dimerization. Molecular Cell, 11(2), 507–517. [https://doi.org/10.1016/s1097-2765\(03\)00047-9](https://doi.org/10.1016/s1097-2765(03)00047-9)

Frezzetti, D., Caridi, V., Marra, L., et al. (2024). The impact of inadequate exposure to epidermal growth factor receptor-tyrosine kinase inhibitors on the development of resistance in non-small-cell lung cancer cells. International Journal of Molecular Sciences, 25(9), 4844. <https://doi.org/10.3390/ijms25094844>

Gou, Q., Gan, X., & Xie, Y. (2024). Novel therapeutic strategies for rare mutations in non-small cell lung cancer. Scientific Reports, 14(1), 10317. <https://doi.org/10.1038/s41598-024-61087-2>

Harris, R. C., Chung, E., & Coffey, R. J. (2003). EGF receptor ligands. Experimental Cell Research, 284(1), 2–13. [https://doi.org/10.1016/s0014-4827\(02\)00105-2](https://doi.org/10.1016/s0014-4827(02)00105-2)

Hubbard, S. R. (1999). Structural analysis of receptor tyrosine kinases. Progress in Biophysics and Molecular Biology, 71(3–4), 343–358. [https://doi.org/10.1016/s0079-6107\(98\)00047-9](https://doi.org/10.1016/s0079-6107(98)00047-9)

Janmaat, M. L., Kruyt, F. A., Rodriguez, J. A., & Giaccone, G. (2003). Response to epidermal growth factor receptor inhibitors in non-small cell lung cancer cells: Limited antiproliferative effects and absence of apoptosis associated with persistent activity of extracellular signal-regulated kinase or Akt kinase pathways. Clinical Cancer Research, 9(6), 2316–2326.

Johnson, M., Garassino, M. C., Mok, T., & Mitsudomi, T. (2022). Treatment strategies and outcomes for patients with EGFR-mutant non-small cell lung cancer resistant to EGFR tyrosine kinase inhibitors: Focus on novel therapies. Lung Cancer, 170, 41–51. <https://doi.org/10.1016/j.lungcan.2022.05.011>

Jura, N., Endres, N. F., Engel, K., et al. (2009). Mechanism for activation of the EGF receptor catalytic domain by the juxtamembrane segment. Cell, 137(7), 1293–1307. <https://doi.org/10.1016/j.cell.2009.04.025>

Lemmon, M. A., & Schlessinger, J. (2010). Cell signaling by receptor tyrosine kinases. Cell, 141(7), 1117–1134. <https://doi.org/10.1016/j.cell.2010.06.011>

Lenferink, A. E. G. (1998). Differential endocytic routing of homo- and hetero-dimeric ErbB tyrosine kinases confers signaling superiority to receptor heterodimers. EMBO Journal, 17(12), 3385–3397. <https://doi.org/10.1093/emboj/17.12.3385>

Mansour, M. A., AboulMagd, A. M., Abbas, S. H., Abdel-Rahman, H. M., & Abdel-Aziz, M. (2023). Insights into fourth generation selective inhibitors of (C797S) EGFR mutation combating non-small cell lung cancer resistance: A critical review. RSC Advances, 13(27), 18825–18853. <https://doi.org/10.1039/d3ra02347h>

Morgillo, F., Della Corte, C. M., Fasano, M., & Ciardiello, F. (2016). Mechanisms of resistance to EGFR-targeted drugs: Lung cancer. ESMO Open, 1(3), e000060. <https://doi.org/10.1136/esmoopen-2016-000060>

Niggenaber, J., Hardick, J., Lategahn, J., & Rauh, D. (2020). Structure defines function: Clinically relevant mutations in ErbB kinases. Journal of Medicinal Chemistry, 63(1), 40–51. <https://doi.org/10.1021/acs.jmedchem.9b00964>

Oxnard, G. R., Lo, P. C., Nishino, M., et al. (2013). Natural history and molecular characteristics of lung cancers harboring EGFR exon 20 insertions. Journal of Thoracic Oncology, 8(2), 179–184. <https://doi.org/10.1097/JTO.0b013e3182779d18>

Reymova, F., Sever, B., Topalan, E., et al. (2025). Design, synthesis, and mechanistic anticancer evaluation of new pyrimidine-tethered compounds. Pharmaceuticals, 18(2), 270. <https://doi.org/10.3390/ph18020270>

Roskoski, R., Jr. (2014). The ErbB/HER family of protein-tyrosine kinases and cancer. Pharmacological Research, 79, 34–74. <https://doi.org/10.1016/j.phrs.2013.11.002>

Roskoski R Jr. Small molecule inhibitors targeting the EGFR/ErbB family of protein-tyrosine kinases in human cancers. Pharmacol Res. 2019 Jan;139:395-411. doi: 10.1016/j.phrs.2018.11.014. Epub 2018 Nov 27. PMID: 30500458.

Sever, B., Altintop, M. D., Radwan, M. O., et al. (2019). Design, synthesis and biological evaluation of a new series of thiazolyl-pyrazolines as dual EGFR and HER2 inhibitors. European Journal of Medicinal Chemistry, 182, 111648. <https://doi.org/10.1016/j.ejmech.2019.111648>

Sever, B., Otsuka, M., Fujita, M., Çiftci, H. (2025) Design, Synthesis, and Anticancer Evaluation of New Small-Molecule EGFR Inhibitors Targeting NSCLC and Breast Cancer. International Journal of Molecular Sciences, 26(15), 7065. <https://doi.org/10.3390/ijms26157065>

Topalan, E., Büyükgüngör, A., Çiğdem, M., Güra, S., Sever, B., Otsuka, M., Fujita, M., Demirci, H., & Çiftci, H. (2025). A structural insight into two important ErbB receptors (EGFR and HER2) and their relevance to non-small cell lung cancer. Archiv der Pharmazie, 358, e2400992. <https://doi.org/10.1002/ardp.202400992>

Wang, K., Fu, Z., Sun, G., et al. (2024). Systemic treatment options for non-small cell lung cancer after failure of previous immune checkpoint inhibitors: A Bayesian network meta-analysis based on randomized controlled trials. *BMC Immunology*, 25(1), 37. <https://doi.org/10.1186/s12865-024-00633-z>

Westover, D., Zugazagoitia, J., Cho, B. C., Lovly, C. M., & Paz-Ares, L. (2018). Mechanisms of acquired resistance to first- and second-generation EGFR tyrosine kinase inhibitors. *Annals of Oncology*, 29(Suppl 1), i10–i19. <https://doi.org/10.1093/annonc/mdx703>

Yarden, Y., & Pines, G. (2012). The ERBB network: At last, cancer therapy meets systems biology. *Nature Reviews Cancer*, 12(8), 553–563. <https://doi.org/10.1038/nrc3309>

Yarden, Y., & Sliwkowski, M. X. (2001). Untangling the ErbB signalling network. *Nature Reviews Molecular Cell Biology*, 2(2), 127–137. <https://doi.org/10.1038/35052073>

Zhao, Y., Wang, H., & He, C. (2021). Drug resistance of targeted therapy for advanced non-small cell lung cancer harbored EGFR mutation: From mechanism analysis to clinical strategy. *Journal of Cancer Research and Clinical Oncology*, 147(12), 3653–3664. <https://doi.org/10.1007/s00432-021-03828-8>